Reznychenko, M., Kotov, D., Bogomaz, O., Zhivolup, T., Reznychenko, A.,
Zalizovski, A., Koloskov, O., Lisachenko, V., & Dzyubanov, D. (2024).
Ionospheric response to the February 27, 2023 intense geomagnetic storm
over Kharkiv and the Akademik Vernadsky station.
Ukrainian Antarctic Journal, *22*(1), 40—50.
https://doi.org/10.33275/1727-7485.1.2024.726

Maryna Reznychenko[1, 2, *], **Dmytro Kotov**[1], **Oleksandr Bogomaz**[1, 3],
Taras Zhivolup[1], **Artem Reznychenko**[2, 4], **Andriy Zalizovski**[2, 3, 4],
Oleksandr Koloskov[3, 4, 5], **Volodymyr Lisachenko**[4], **Dmytro Dzyubanov**[6]

[1] Institute of Ionosphere, National Academy of Sciences of Ukraine and Ministry of Education and Science of Ukraine, Kharkiv, 61001, Ukraine
[2] Space Research Centre of Polish Academy of Sciences, Warsaw, 00-716, Poland
[3] State Institution National Antarctic Scientific Center, Ministry of Education and Science of Ukraine, Kyiv, 01601, Ukraine
[4] Institute of Radio Astronomy, National Academy of Sciences of Ukraine, Kharkiv, 61002, Ukraine
[5] University of New Brunswick, Fredericton, New Brunswick, E3B5A3, Canada
[6] National Technical University “Kharkiv Polytechnic Institute”, Kharkiv, 61002, Ukraine

*** Corresponding author:** marina.shulga23@gmail.com

Ionospheric response to the February 27, 2023 intense geomagnetic storm over Kharkiv and the Akademik Vernadsky station

---

Abstract. This study aims to investigate ionospheric responses to the February 27, 2023 intense geomagnetic storm over Kharkiv and the Akademik Vernadsky (hereinafter — Vernadsky) station using ionosondes. The behavior of the key ionospheric parameters (h_{mF2} and N_{mF2}) before, during, and after the geomagnetic storm was investigated. The observational F2-layer peak electron density and height were compared with those derived by the International Reference Ionosphere (IRI-2016) model. Significant negative ionospheric storms were identified over Kharkiv during all the nights after the geomagnetic storm beginning (up to ~70% decrease of the N_{mF2}). At the same time, during the daytime hours of February 27, a moderate positive ionospheric storm (up to ~40% increase of the N_{mF2}) was registered. Over Vernadsky Station, during the main phase of the geomagnetic storm, a very strong negative ionospheric storm (up to a factor of ~4 reduction of the N_{mF2}) was observed both during daytime and night-time. We offer hypotheses of the possible physical mechanisms (electrodynamics, changes in the neutral composition, partial depletion of the plasmasphere, and a shift of the ionospheric trough) responsible for the observed ionospheric effects. Further investigations with physical models of the coupled atmosphere, ionosphere, and plasmasphere are necessary to identify the dominant drivers in each case. Comparison of the observed ionospheric parameters with the predictions of IRI F2-layer peak sub-models shows that neither h_{mF2} (AMTB-2013 and SHU-2015), and N_{mF2} (URSI and CCIR) sub-models can qualitatively reproduce strong storm-induced ionospheric variations over Kharkiv. Over Vernadsky Station, both h_{mF2} sub-models underestimate the observed h_{mF2} during the storm period, whereas the N_{mF2} sub-models are more sensitive to the changes in geomagnetic activity. Under geomagnetically quiet conditions, the qualitative agreement between observations and the model is satisfactory, but further improvements of the empirical models are required to reach acceptable accuracy of quantitative predictions.

Keywords: electron density, empirical model, F2-layer peak height, geomagnetic storm, ionosonde, ionosphere

---

1 Introduction

Although the ionospheric effects of geomagnetic storms have been actively investigated for decades and the key physical mechanisms responsible for them have been found, every storm has its unique features and effects, which cannot be fully reproduced by the existing empirical models (Prölss, 2008; Fuller-Rowell, 2011; Borries et al., 2015). More observations of new storms and additional comparisons with the models are required to improve the models further.

The February 27–28, 2023 geomagnetic storm is particularly interesting for models' testing. The storm occurred at relatively high solar activity ($F_{10.7}$ ~160), the highest for the last ~20 years. During this period, new empirical models for the F2-layer peak height ($h_{m\mathrm{F2}}$) have been developed and are widely used as commonly accepted options of the International Reference Ionosphere (IRI) model (Bilitza et al., 2017; 2022). However, there is a lack of studies devoted to testing the accuracy of these models under high solar activity conditions over Antarctica compared to other regions of the Earth. Furthermore, it is unclear whether the standard IRI models of the F2-layer peak electron density ($N_{m\mathrm{F2}}$) based on the data obtained for previous solar cycles can predict $N_{m\mathrm{F2}}$ during the maximum of the current 25th solar cycle with acceptable accuracy.

This study focuses on such validation efforts. We analyse variations of the ionospheric F2-layer peak in mid-latitudes of the European longitudinal sector, Northern Hemisphere, and in the sub-auroral latitudes of the American longitudinal sector, Southern Hemisphere, during the period of 25–28 February 2023, which encompasses the pre-storm days, main storm phase, and beginning of the recovery phase.

We employ observations by ionosondes at Kharkiv (49.6°N, 36.3°E) and the Ukrainian Antarctic Akademik Vernadsky (hereinafter – Vernadsky) station (65.25°S, 295.75°E) and compare them with AMTB-2013 and SHU-2015 sub-models for $h_{m\mathrm{F2}}$ and CCIR and URSI sub-models for $N_{m\mathrm{F2}}$ (Zalizovski et al., 2018; Koloskov et al., 2019; 2023; Bilitza et al., 2022).

This paper is structured as follows: The first section provides a short overview of the problem associated with ionospheric modeling under high solar and geomagnetic activity levels. The second section describes the space weather conditions, data, and methods used in this paper. The results and discussions are presented in the third section. The last section concludes the paper.

2 Data and methods

2.1 Solar and geomagnetic conditions

Figure 1 shows variations in solar and geomagnetic activity indices from February 25 to 28, 2023. The solar activity during the investigated period ranged from medium to high level (solar radio flux index $F_{10.7}$ = 152–161 sfu). Geomagnetic activity was enhanced from ~18:00 UT on February 26 to 03:00 UT on February 28 with a maximum value of the planetary index of geomagnetic activity K_{pmax} = 7– on February 27; the rest of the period was relatively quiet (K_p did not exceed 4). According to the National Oceanic and Atmospheric Administration (NOAA) Geomagnetic Storm Scale, the February 27, 2023 geomagnetic storm was classified as G3 (Strong) event. The symmetric disturbance of the horizontal component of the geomagnetic field (SYM/H index) reached −161 nT around February 27 noon, which indicates significant ring current disturbances.

2.2 Ionosonde measurements

The data used in the paper were obtained by three ionosondes, two located at Vernadsky Station and one at the Observatory of the Institute of Ionosphere 50 km southeast of Kharkiv (near the city of Zmiiv).

The hardware and software of the IPS-42 and SDR-based ionosondes operating at Vernadsky Station are described in (Broom, 1984) and (Koloskov et al., 2023). The modified ionosonde VISRC-2t, operating at the Observatory of the Institute of

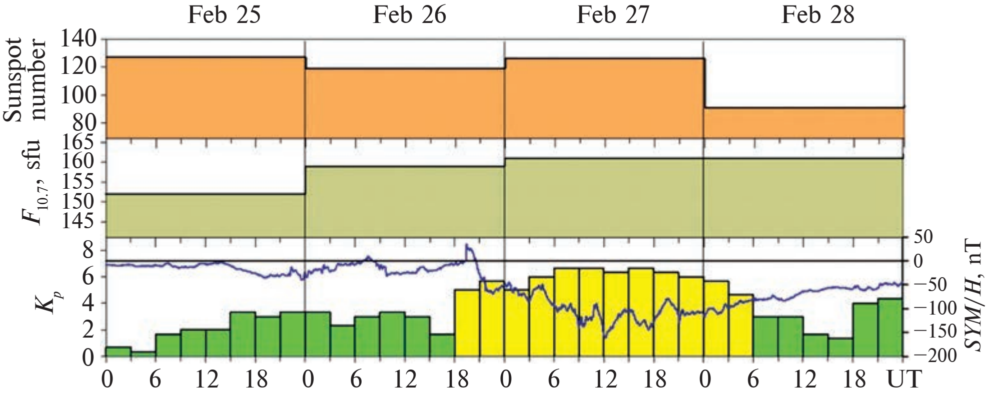

Figure 1. Variations of the parameters describing the solar and geomagnetic conditions during February 25–28, 2023. The panels from top to bottom display the daily sunspot numbers, the daily value of the solar activity index $F_{10.7}$, the 3-hour K_p index (green and yellow bars indicate low and moderate levels of geomagnetic activity, respectively), and the SYM/H index (blue solid line). The time is UTC

Ionosphere, has a transmission power of about 400 W, uses Barker-coded pulses, and provides sounding every minute (due to the high complexity of manual processing of ionograms, the current research is based on data obtained at 5-minute intervals).

More parameters of the ionosondes' operating mode are listed in Table.

Ionograms of all three ionosondes were manually scaled using IonogramViewer2 version 1.6.3 (https://github.com/Albom/IonogramViewer2/releases/download/v1.6.3/IonogramViewer2-1.6.3.zip). The obtained critical frequencies of F2, F1, and E layers and traces were used for electron density profile inversion using NHPC program version 4.30 (Huang & Reinisch, 1996) and further calculation of the F2-layer peak height. The validity of such a technique was proven by a number of investigations (Bogomaz et al., 2019; Shulha et al., 2019; Reznychenko et al., 2022; 2023). Due to the time-consuming process of the ionogram scaling, the calculation of h_{mF2} over the Antarctic Peninsula was performed only using the SDR-based ionosonde data. It should also be noted that some lack of echoes in the ionograms from both ionosondes at Vernadsky Station (SDR and IPS-42) was detected during a strong storm period on February 27, 2023. The probable reason for such complete or partial radio signal fade-out was the intense absorption of high-frequency (HF) radio waves. Such ionograms were discarded from the analysis.

2.3 F2-layer peak models

In this study, we compare the ionosonde observations with the F2-layer peak electron density

Table. Operating mode parameters of the ionosondes

Parameter	The SDR-based ionosonde	IPS-42 ionosonde	The modified VISRC-2t ionosonde
Frequency range	1–16 MHz	1–22.6 MHz	1–16 MHz
Number of frequencies	320	576	750
Virtual height range	92–655 km	0–800 km	80–800 km
Total heights	750	512	1110
Transmitter pulse width	600 μs (16 × 37.5 μs)	41.7 μs	455 μs (13 × 35 μs)

and height ($h_{m\mathrm{F2}}$ and $N_{m\mathrm{F2}}$) predictions for the same dates by sub-models of the IRI-2016 model (Bilitza et al., 2017; 2022). The Comité Consultatif International pour la Radio (CCIR) (International Radio Consultative Committee, 1967) and Union Radio Scientifique Internationale (URSI) (Rush et al., 1989) sub-models were used to obtain $N_{m\mathrm{F2}}$. Both $N_{m\mathrm{F2}}$ sub-models depend on the solar activity indices and were configured with the "foF2 STORM model" option (Fuller-Rowell et al., 2000), which was activated for this study. The SHU-2015 (Shubin, 2015) and AMTB-2013 (Altadill et al., 2013) sub-models were used to obtain $h_{m\mathrm{F2}}$. Both $h_{m\mathrm{F2}}$ sub-models are also governed by solar activity indices but insensitive to changes of the magnetic activity.

3 Results and discussion

3.1 Results of observations over Kharkiv and Vernadsky Station

Figure 2 shows diurnal variations of the key ionospheric parameters ($h_{m\mathrm{F2}}$ and $N_{m\mathrm{F2}}$) obtained using ionosondes at Kharkiv and Vernadsky Station and calculated by the IRI-2016 model. It can be seen that for the period of February 26–28, the $N_{m\mathrm{F2}}$ trends obtained with the SDR-based ionosonde and IPS-42 demonstrate a good agreement in determining the critical frequencies (f_{oF2}) and complement each other.

3.1.1 Variations of the F2-layer peak parameters over Kharkiv. It is worth mentioning that variations of both peak electron density and peak height over Kharkiv are representative of high solar activity conditions. The $h_{m\mathrm{F2}}$ and $N_{m\mathrm{F2}}$ values are significantly higher than those obtained for the same region, local time, and near seasons under low solar activity conditions (e.g., Kotov et al., 2016; 2018; Panasenko et al., 2021). The smallest values of $h_{m\mathrm{F2}}$ were ~250 km, and they appeared in the early morning hours as expected (Prölss, 2004). Then, $h_{m\mathrm{F2}}$ values increased until reaching a daytime maximum around noon (~280 km during quiet geomagnetic conditions, while for the disturbed day on February 27, $h_{m\mathrm{F2max}}$ was ~310 km). On February 25, around sunset, $h_{m\mathrm{F2}}$ values experienced a reduction of ~5–10 km and then started to increase at ~16:30 UT and reached a maximum of ~425 km by ~18 UT. On February 26, the post-sunset increase of $h_{m\mathrm{F2}}$ also started at 16:30 UT, but reached the maximum (~ 470 km) ~3 hours later than the previous day. On February 27, by 18 UT, $h_{m\mathrm{F2}}$ reached ~525 km. On February 28, during the storm's recovery phase, $h_{m\mathrm{F2}}$ variations closely mirrored those on February 25. Similar variations were independently observed by ionosondes in the European region (Bojilova & Mukhtarov, 2023; Aa et al., 2023).

The daytime uplift of the F2 layer in the early hours of February 27 caused a positive ionospheric storm: a ~40% increase of $N_{m\mathrm{F2}}$ (from ~7 to ~14 UT) compared to the corresponding period of a geomagnetically quiet day on February 25. The uplift could result from daytime penetration of the eastward electric field (e.g., Kotov et al., 2019).

Significant negative ionospheric storms (~70% decrease of $N_{m\mathrm{F2}}$ compared with the pre-storm values on February 25) were seen during all three nights after the magnetic storm started. During the first night (February 26–27), the $N_{m\mathrm{F2}}$ reduction was probably caused by the mid-latitude ionospheric trough's motion towards lower latitudes (Matyjasiak et al., 2016) or by partial depletion of the plasmasphere, which led to the reduction of the downward H^+ ion flux which is responsible for the increase of $N_{m\mathrm{F2}}$ at middle latitudes during winter nights (Kotov et al., 2016; 2018). Enhanced recombination by increased molecular nitrogen density is not a likely cause because not enough time had passed since the storm's beginning. During the second night (February 27–28) and the third night (February 28–29), all three mentioned factors could contribute to the $N_{m\mathrm{F2}}$ reduction.

In general, the changes observed during the geomagnetically disturbed period over Kharkiv are consistent with the existing knowledge regarding the effects of geomagnetic storms on the ionosphere. In particular, the effects of the penetra-

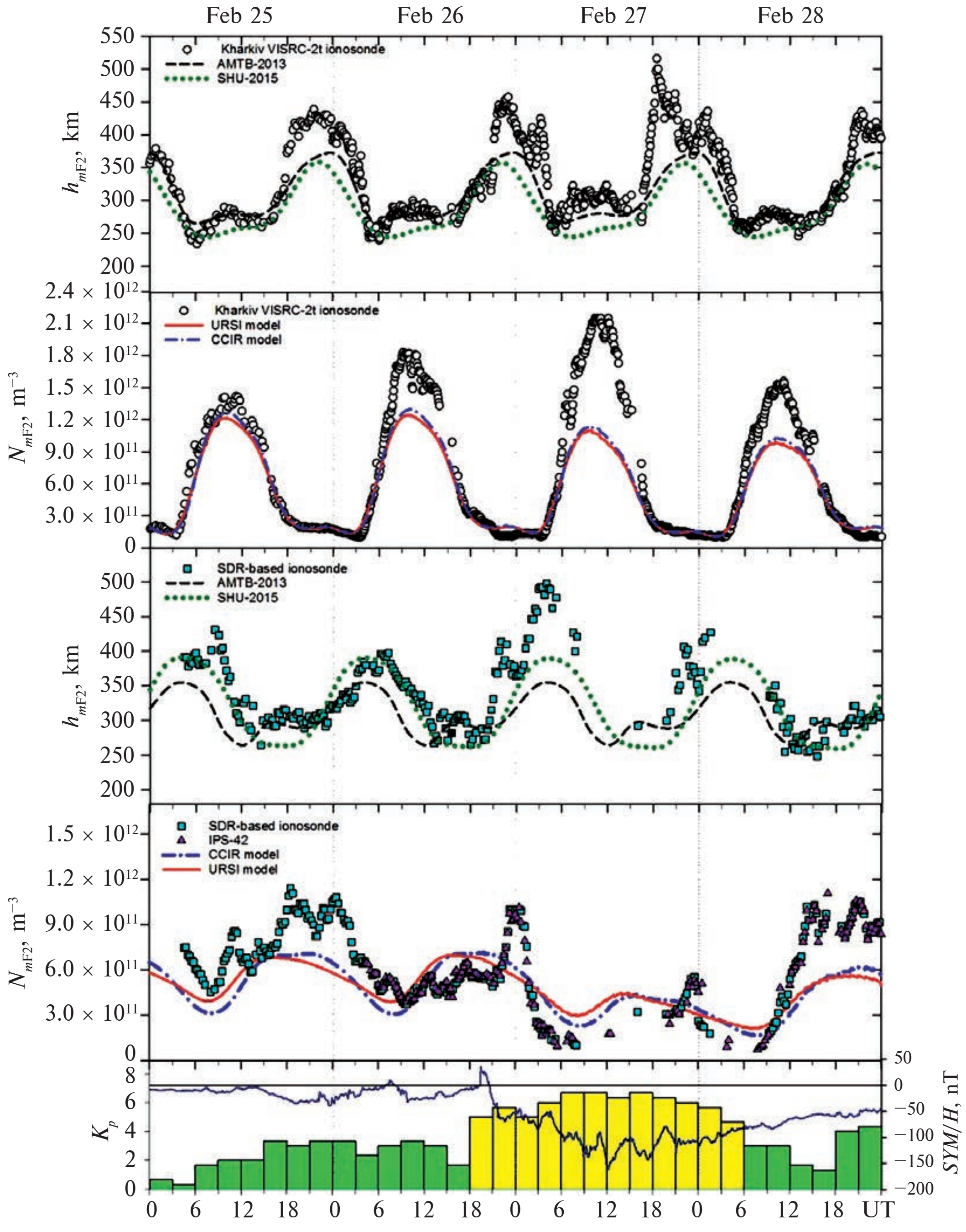

Figure 2. Comparison of the experimental results obtained for Kharkiv and Vernadsky Station with the IRI-2016 model values during February 25–28, 2023. Open circles show the VISRC-2t ionosonde data (Kharkiv). Full blue squares denote the SDR-based ionosonde data (Vernadsky Station). Full pink triangles denote the IPS-42 ionosonde data (Vernadsky Station). The dotted green lines show h_{mF2} variations from the SHU-2015 sub-model, and the dashed black lines are from the AMTB-2013 sub-model. The solid red lines show N_{mF2} variations from the URSI sub-model, and the dot-dashed blue lines are from the CCIR sub-model. The time for the considered stations is $UT_{Kharkiv} \approx$ LT-2hours and $UT_{Vernadsky} \approx$ LT+4hours

tion of short-time electric fields of magnetospheric origin, heated neutral atmosphere (Prölss, 2004; Arslan Tariq et al., 2024), and partially depleted plasmasphere (e.g., Kotov et al., 2018). A more detailed analysis of the possible physical mechanisms responsible for the effects observed in the ionosphere over Kharkiv for this event will be the subject of further work.

3.1.2 Variations of F2-layer peak parameters over Vernadsky Station. Regular variations of F2-layer peak parameters at Vernadsky Station differ from those at Kharkiv. It should be noted that February is the end of Antarctica's local summer, when the ionosphere is sunlit most of the day, which is in contrast with the winter conditions over Kharkiv.

Given the larger tilt of the Earth's magnetic field in the sub-auroral latitudes, even small enhancements of high-latitude convection, which typically occurs permanently at low enough magnetic activity ($K_p > 2$), can have a noticeable effect on the variations of $h_{m\mathrm{F2}}$ and $N_{m\mathrm{F2}}$ parameters over Vernadsky Station. Hence, the $N_{m\mathrm{F2}}$ behavior is much more variable than that for Kharkiv, even within the pre-storm period of February 25–26.

Unfortunately, due to the strong ionospheric absorption of the ionosonde radio signals, there are no data for Vernadsky Station for most of the storm period of February 27. Nevertheless, examining the accessible data reveals that, in contrast to Kharkiv, a strong negative ionospheric storm developed during the daytime of February 27 (both for SDR-based ionosonde and IPS-42). The main source of such a strong (up to a factor of 4) reduction of $N_{m\mathrm{F2}}$ is likely a decrease in $\mathrm{O/N_2}$ ratio caused by the increased thermosphere temperature in high latitudes by enhanced Joule heating and precipitation of particles in the auroral zone (Prölss, 2004). The equatorward shifts of the mid-latitude ionospheric trough by enhanced high-latitude convection can be an additional possible reason for strong negative ionospheric storms (a decrease in $N_{m\mathrm{F2}}$ at least 3 to 4 times) observed during the nights of February 27 and 28 (Yang et al., 2022).

3.2 Comparison of observations with empirical model predictions

Figure 2 shows that the IRI $h_{m\mathrm{F2}}$ sub-models represent the average behavior of $h_{m\mathrm{F2}}$ and are insensitive to the storm over both Kharkiv and Vernadsky Station. This is unsurprising for the $h_{m\mathrm{F2}}$ models because they are independent of the magnetic activity and governed by the $F_{10.7}$ index only. The IRI $N_{m\mathrm{F2}}$ sub-models reproduce the ionospheric storm effects over the Antarctic Peninsula very well. At the same time, they do not show the real storm-related changes in variations of $N_{m\mathrm{F2}}$ for mid-latitudes of the European region despite the "STORM" option being turned on.

3.2.1 Results of comparison for Kharkiv. The SHU-2015 sub-model shows poor agreement with the $h_{m\mathrm{F2}}$ observations over Kharkiv, even for the pre-storm days, both during daytime and night-time. The AMTB-2013 sub-model agrees better with the observations during the daytime before and after the storm-timed period (on February 25, 26, and 28, respectively). In contrast, during the daytime of the disturbed period (February 27), AMTB-2013 underestimates the $h_{m\mathrm{F2}}$ values by ~30 km. During the night-time, AMTB predictions are unsatisfactory. Discrepancies between the observations and sub-model predictions vary from ~50 to ~200 km, depending on the level of geomagnetic activity.

Both the IRI $N_{m\mathrm{F2}}$ sub-models (URSI and CCIR) provide quite good qualitative agreement with the Kharkiv ionosonde observations during the daytime and night-time of the pre-storm day of February 25. At the same time, large discrepancies (~2 times) are seen for the night-time periods of February 26 and 28 and during the daytime of the disturbed period (February 27). Notable differences between the observations and sub-model predictions are also seen during the daytime of February 26 and 28, when the $N_{m\mathrm{F2}}$ sub-models underestimate the $N_{m\mathrm{F2}}$ by ~35%.

3.2.2 Results of comparison for Vernadsky Station. The F2-layer peak height predictions obtained by the AMTB-2013 sub-model are more consistent with the daytime observations than the

SHU-2015 sub-model. The latter, in turn, shows a better agreement with observations during the night-time of quiet days. Both $h_{m\mathrm{F2}}$ sub-models significantly (by ~100 km for SHU-2015 and ~120 km for AMTB-2013) underestimate the F2-layer peak height during the disturbed period of February 27.

The IRI $N_{m\mathrm{F2}}$ sub-models provide a relatively good agreement with the daytime Vernadsky ionosonde observations, including the intense storm period. Unfortunately, large gaps in the ionosonde data for February 27 do not allow to draw detailed conclusions on the observations/model differences for the storm day. At the same time, some underestimations (by ~40%) during the afternoon hours for the pre-storm and post-storm days of February 25 and 28 are observed, as well as in the evening hours (around 22:00 UT) at the onset of the geomagnetic storm on February 26.

4 Conclusions

The behavior of the key ionospheric parameters (F2-layer peak electron density and height before, during, and after the strong (K_{pmax}=7−) magnetic storm of February 27, 2023, was investigated using the data from ionosondes located at Kharkiv and Vernadsky Station. The main results are as follows:

1. Over Kharkiv, significant negative ionospheric storms (up to ~70% decrease of the $N_{m\mathrm{F2}}$) were observed during all nights after the storm's beginning. A moderate positive ionospheric storm (up to ~40% increase of the $N_{m\mathrm{F2}}$) occurred during the main phase of the magnetic storm in the daytime of February 27.

2. Over Vernadsky Station, the $N_{m\mathrm{F2}}$ behavior was much more variable than that for Kharkiv, even within the pre-storm period of February 25–26. Despite data gaps for most of the storm period for Vernadsky Station on February 27, a very strong negative ionospheric storm (up to a factor of ~4 reduction of the $N_{m\mathrm{F2}}$) was detected during the daytime. Strong negative ionospheric storms (a decrease in $N_{m\mathrm{F2}}$ at least 3 to 4 times) were observed during the nights of February 27 and 28.

3. The results of observations over both Kharkiv and Vernadsky Station agree well with the current understanding of the magnetic storms' impact on the ionosphere. The vertical and horizontal motion of the ionosphere driven by penetration of the magnetospheric electric field, changes in the neutral composition, and partial depletion of the plasmasphere, which all were caused by the magnetic storm, are speculated as the likely key drivers of the observed ionospheric storms. Further investigations with physical models of the coupled atmosphere, ionosphere, and plasmasphere are needed to understand which drivers were dominant in each case.

4. Comparison of ionospheric parameters obtained by ionosondes with predictions by the modern sub-models of the International Reference Ionosphere model shows that neither $h_{m\mathrm{F2}}$ nor $N_{m\mathrm{F2}}$ sub-models can qualitatively reproduce storm-induced changes in the ionosphere over Kharkiv. Over Vernadsky Station, the AMTB-2013 model showed a better agreement with the daytime observations, whereas the SHU-2015 agrees well with measurements during the night-time of quiet days. At the same time, both $h_{m\mathrm{F2}}$ sub-models significantly underestimate the observed $h_{m\mathrm{F2}}$ during the storm period, especially because, for this ionospheric parameter, the IRI model does not provide a "STORM" option. On the contrary, the IRI $N_{m\mathrm{F2}}$ sub-models, for which a "STORM" option is provided, are more sensitive to the geomagnetic activity changes. The reproducing of the quiet-time variations is good enough qualitatively. However, more improvements of the empirical models are still needed to achieve acceptable accuracy in quantitative predictions.

Data and software. The IonogramViewer2 program can be downloaded from the repository on GitHub (retrieved December 5, 2023 from https://github.com/Albom/IonogramViewer2). The NHPC program can be downloaded from the UMass Lowell Space Science Lab website (retrieved December 5, 2023 from https://ulcar.uml.edu/SoftwareUtilities/NHPC/NHPC430.ZIP). International Reference Ionosphere (2016) online version is available on the Community Coordinated Modeling Center website (retrieved December 15, 2023, https://ccmc.gsfc. nasa.gov/modelweb/models/iri2016_vitmo.php). Sunspot number data are provided by Solar Influences Data Analysis Center (a part of the Royal Observatory of Belgium) and available on SIDC website (retrieved December 5, 2023 from http://www.sidc.be/silso/DATA/SN_d_tot_V2.0.txt). The K_p index was obtained from the World Data Center for Geomagnetism (https://wdc.kugi.kyoto-u.ac.jp/aedir/), $F_{10.7}$ solar flux index via FTP Server (retrieved June 19, 2024, ftp://ftp.swpc.noaa.gov/pub/indices/old_indices/), SYM/H index was taken from the OMNIWeb (retrieved December 5, 2023, https://omniweb.gsfc.nasa.gov/form/omni_min.html).

Author contributions. The idea, data processing, and illustration preparing: O.B., M.R., D.K. and T.Z. Data acquisition and preparation: O.B., A.R., O.K. and V.L. Simulations: M.R. Interpretation of the results: M.R. and D.K. Writing: M.R., D.K. and O.B. Manuscript review and editing: M.R., D.K., O.B., A.Z., O.K., D.D. All authors have read and agree to publish the current version of the manuscript.

Acknowledgments. The authors are sincerely grateful to all defenders of Ukraine for the opportunity for Ukrainian scientists to continue their research activities.

Funding. The study was done in the framework of the grant 0123U103637 “Development of deep neural networks for detecting and estimating parameters of atmospheric gravity waves and travelling ionospheric disturbances” financed by the State Institution National Antarctic Scientific Center of the Ministry of Education and Science of Ukraine in 2023. OB, MR, AR and AZ were also supported by the long-term program of support for Ukrainian research teams at the Polish Academy of Sciences, carried out in cooperation with external partners (agreement number PAN.BFB.S.BWZ.364.022.2023). OB, MR, DK also acknowledge the EOARD — STCU Partner Project P795 “Diagnostics of natural and manmade ionospheric disturbances over Ukraine”, AR, AZ, OK, VL acknowledge the EOARD — STCU Partner Project P775 (EOARD 22IOE019).

Conflict of Interest. The authors declare no conflict of interest.

References

Aa, E., Zhang, S.-R., Wang, W., Erickson, P. J., & Coster, A. J. (2023). Multiple longitude sector storm-enhanced density (SED) and long-lasting subauroral polarization stream (SAPS) during the 26—28 February 2023 geomagnetic storm. *Journal of Geophysical Research: Space Physics*, *128*(9), e2023JA031815. https://doi.org/10.1029/2023JA031815

Altadill, D., Magdaleno, S., Torta, J. M., & Blanch, E. (2013). Global empirical models of the density peak height and of the equivalent scale height for quiet conditions. *Advances in Space Research, 52*(10), 1756—1769. https://www.doi.org/10.1016/j.asr.2012.11.018

Arslan Tariq, M., Liu, L., Shah, M., Yang, Y., Sun, W., Ali Shah, M., Zhang, R., & Yoshikawa, A. (2024) Longitudinal variations of ionospheric responses to the February and April 2023 geomagnetic storms over American and Asian sectors. *Advances in Space Research*, *73*(6), 3033—3049. https://doi.org/10.1016/j.asr.2023.12.039

Bilitza, D., Altadill, D., Truhlik, V., Shubin, V., Galkin, I., Reinisch, B., & Huang, X. (2017). International reference ionosphere 2016: From ionospheric climate to real-time weather predictions. *Space Weather*, *15*(2), 418—429. https://doi.org/10.1002/2016SW001593

Bilitza, D., Pezzopane, M., Truhlik, V., Altadill, D., Reinisch, B. W., & Pignalberi, A. (2022). The International Reference Ionosphere model: a review and description of an ionospheric benchmark. *Reviews of Geophysics*, *60*(4), e2022RG000792. https://doi.org/10.1029/2022RG000792

Bogomaz, O. V., Shulha, M. O., Kotov, D. V., Zhivolup, T. G., Koloskov, A. V., Zalizovski, A. V., Kashcheyev, S. B., Reznychenko, A. I., Hairston, M. R., & Truhlik, V. (2019). Ionosphere over Ukrainian Antarctic Akademik Vernadsky station under minima of solar and magnetic activities, and daily insolation: case study for June 2019. *Ukrainian Antarctic Journal*, (2(19), 84—93. https://doi.org/10.33275/1727-7485.2(19).2019.154

Bojilova, R., & Mukhtarov, P. (2023). Analysis of the ionospheric response to Sudden Stratospheric Warming and geomagnetic forcing over Europe during February and March 2023. *Universe, 9*(8), 351. https://doi.org/10.3390/universe9080351

Borries, C., Berdermann, J., Jakowski, N., & Wilken, V. (2015). Ionospheric storms — a challenge for empirical forecast of the total electron content. *Journal of Geophysical Research: Space Physics*, *120*(4), 3175–3186. https://doi.org/10.1002/2015JA020988

Broom, S. M. (1984). A new ionosonde for Argentine Islands ionospheric observatory, Faraday Station. *British Antarctic Survey Bulletin*, 62, 1–6. http://nora.nerc.ac.uk/id/eprint/523821/

Fuller-Rowell, T. J. (2011). Storm–time response of the thermosphere–ionosphere system. In M. A. Abdu, & D. Pancheva (Eds.), *Aeronomy of the Earth's Atmosphere and Ionosphere* (Vol. 2, pp. 419–435). Springer. https://doi.org/10.1007/978-94-007-0326-1_32

Fuller-Rowell, T. J., Araujo-Pradere, E., & Codrescu, M. V. (2000). An empirical ionospheric storm-time correction model. *Advances in Space Research*, *25*(1), 139–146. https://doi.org/10.1016/S0273-1177(99)00911-4

Huang, X., & Reinisch, B. W. (1996). Vertical electron density profiles from the Digisonde network. *Advances in Space Research*, *18*(6), 121–129. https://doi.org/10.1016/0273-1177(95)00912-4

International Radio Consultative Committee (CCIR). (1967). CCIR Atlas of ionospheric characteristics. (Report No. 340). *International Telecommunication Union*. https://search.itu.int/history/HistoryDigitalCollectionDocLibrary/4.281.43.es.3019.pdf

Koloskov, O., Kashcheyev, A., Bogomaz, O., Sopin, A., Gavrylyuk, B., & Zalizovski, A. (2023). Performance analysis of a portable low-cost SDR-based ionosonde. *Atmosphere*, *14*(1), 159. https://doi.org/10.3390/atmos14010159

Koloskov, O. V., Kashcheyev, A. S., Zalizovski, A. V., Kashcheyev, S. B., Budanov, O. V., Charkina, O. V., Pikulik, I. I., Lysachenko, V. M., Sopin, A. O., & Reznychenko, A. I. (2019). New digital ionosonde developed for Akademik Vernadsky station. In *Book of Abstracts "IX International Antarctic Conference dedicated to the 60th anniversary of the signing of the Antarctic Treaty in the name of peace and development of international cooperation: Physical sciences"* (Kyiv, 14–16 May, 2019, pp. 170–171). http://uac.gov.ua/international-cooperation/mak/mak-2019/

Kotov, D. V., Richards, P. G., Bogomaz, O. V., Chernogor, L. F., Truhlík, V., Emelyanov, L. Ya., Chepurnyy, Ya. M., & Domnin, I. F. (2016). The importance of neutral hydrogen for the maintenance of the midlatitude winter nighttime ionosphere: evidence from IS observations at Kharkiv, Ukraine, and field line interhemispheric plasma model simulations. *Journal of Geophysical Research: Space Physics*, *121*(7), 7013–7025. https://doi.org/10.1002/2016JA022442

Kotov, D. V., Richards, P. G., Truhlík, V., Bogomaz, O. V., Shulha, M. O., Maruyama, N., Hairston, M., Miyoshi, Y., Kasahara, Y., Kumamoto, A., Tsuchiya, F., Matsuoka, A., Shinohara, I., Hernández-Pajares, M., Domnin, I. F., Zhivolup, T. G., Emelyanov, L. Ya., & Chepurnyy, Ya. M. (2018). Coincident observations by the Kharkiv IS radar and ionosonde, DMSP and Arase (ERG) Satellites, and FLIP model simulations: implications for the NRLMSISE-00 hydrogen density, plasmasphere, and ionosphere. *Geophysical Research Letters*, *45*(16), 8062–8071. https://doi.org/10.1029/2018GL079206

Kotov, D. V., Richards, P. G., Truhlík, V., Maruyama, N., Fedrizzi, M., Shulha, M. O., Bogomaz, O. V., Lichtenberger, J., Hernández-Pajares, M., Chernogor, L. F., Emelyanov, L. Ya., Zhivolup, T. G., Chepurnyy, Ya. M., & Domnin, I. F. (2019). Weak magnetic storms can modulate ionosphere-plasmasphere interaction significantly: mechanisms and manifestations at mid-latitudes. *Journal of Geophysical Research: Space Physics, 124,* 9665–9675. https://doi.org/10.1029/2019JA027076

Matyjasiak, B., Przepiórka, D., & Rothkaehl, H. (2016). Seasonal variations of mid-latitude ionospheric trough structure observed with DEMETER and COSMIC. *Acta Geophysica,* 64, 2734–2747. https://doi.org/10.1515/acgeo-2016-0102

Panasenko, S. V., Kotov, D. V., Otsuka, Y., Yamamoto, M., Hashiguchi, H., Richards, P. G., Truhlik, V., Bogomaz, O. V., Shulha, M. O., Zhivolup, T. G., & Domnin, I. F. (2021). Coupled investigations of ionosphere variations over European and Japanese regions: observations, comparative analysis, and validation of models and facilities. *Progress in Earth and Planetary Science*, 8, 45. https://doi.org/10.1186/s40645-021-00441-8

Prölss, G. W. (2004). *Physics of the Earth's space environment. An Introduction* (1st ed.). Springer Berlin Heidelberg. https://doi.org/10.1007/978-3-642-97123-5

Prölss, G. W. (2008). Ionospheric storms at mid-latitude: a short review. In P. M. Kintner Jr., A. J. Coster, T. Fuller-Rowell, A. J. Mannucci, M. Mendillo, & R. Heelis (Eds.), *Midlatitude Ionospheric Dynamics and Disturbances* (Vol. 181, pp. 9–24). AGU, Washington, D. C. htts://doi.org/10.1029/181GM03

Reznychenko, M., Bogomaz, O., Kotov, D., Zhivolup, T., Koloskov, O., & Lisachenko, V. (2022). Observation of the ionosphere by ionosondes in the Southern and Northern hemispheres during geospace events in October 2021. *Ukrainian Antarctic Journal*, *20*(1(24), 18–30. https://doi.org/10.33275/1727-7485.1.2022.686

Reznychenko, M. O., Kotov, D. V., Bogomaz, O. V., Koloskov, O. V., & Lisachenko, V. M. (2023). Ionospheric response to some moderate geomagnetic storms over the Ukrainian Antarctic station and magnetically conjugated region. In Book of Abstracts *"XI International Antarctic Conference dedicated to the 160th anniversary of the birth of Volodymyr Vernadsky — the first president of the Ukrainian Academy of Sciences, founder of the study of Noosphere"* (Kyiv, 10–12 May, 2023, pp. 65–66). http://uac.gov.ua/wp-content/uploads/2023/05/Book-of-Abstracts_IAC-11_2023_.pdf

Rush, C., Fox, M., Bilitza, D., Davies, K., McNamara, L., Stewart, F., & PoKempner, M. (1989). Ionospheric mapping — An update of foF2 coefficients. *Telecommunications Journal*, *56*(3), 179—182.

Shubin, V. N. (2015). Global median model of the F2-layer peak height based on ionospheric radio-occultation and ground-based Digisonde observations. *Advances in Space Research*, *56*(5), 916—928. https://doi.org/10.1016/j.asr.2015.05.029

Shulha, M. O., Kotov, D. V., Bogomaz, O. V., Zhivolup, T. G., Koloskov, O. V., Lisachenko, V. M., & Hairston, M. (2019). Multi-instrumental and modeling investigation of ionospheric response to weak geomagnetic storm of 21—23 March 2017 over the Ukrainian Antarctic station and magnetically conjugate region. In *Book of Abstracts "IX International Antarctic Conference dedicated to the 60th anniversary of the signing of the Antarctic Treaty in the name of peace and development of international cooperation"* (Kyiv, 14—16 May, 2019, pp. 185—186). http://uac.gov.ua/international-cooperation/mak/mak-2019/

Yang, N., Yu, T., Le, H., Liu, L., Sun, Y.-Y., Yan, X., Wang, J., Xia, C., Zuo, X., & Huang, G. (2022). The feature of ionospheric mid-latitude trough during geomagnetic storms derived from GPS Total Electron Content (TEC) data. *Remote Sensing*, *14*(2), 369. https://doi.org/10.3390/rs14020369

Zalizovski, A. V., Kashcheyev, A. S., Kashcheyev, S. B., Koloskov, A. V., Lisachenko, V. N., Paznukhov, V. V., Pikulik, I. I., Sopin, A. A., & Yampolski, Yu. M. (2018). A prototype of a portable coherent ionosonde model. *Space Science and Technology*, *24*(3), 10—22. https://doi.org/10.15407/knit2018.03.010

Received: 26 December 2023
Accepted: 13 July 2024

Марина Резниченко[1, 2, *], Дмитро Котов[1], Олександр Богомаз[1, 3], Тарас Живолуп[1], Артем Резниченко[2, 4], Андрій Залізовський[2, 3, 4], Олександр Колосков[3, 4, 5], Володимир Лисаченко[4], Дмитро Дзюбанов[6]

[1] Інститут іоносфери Національної академії наук України та Міністерства освіти і науки України, м. Харків, 61001, Україна
[2] Центр космічних досліджень Польської академії наук, м. Варшава, 00-716, Польща
[3] Державна установа Національний антарктичний науковий центр Міністерства освіти і науки України, м. Київ, 01601, Україна
[4] Радіоастрономічний інститут Національної академії наук України, м. Харків, 61002, Україна
[5] Університет Нью-Брансвік, м. Фредеріктон, Нью-Брансвік, E3B5A3, Канада
[6] Національний технічний університет «Харківський політехнічний інститут», м. Харків, 61002, Україна

*** Автор для кореспонденції:** marina.shulga23@gmail.com

Реакція іоносфери на інтенсивну геомагнітну бурю 27 лютого 2023 року над Харковом та станцією «Академік Вернадський»

Реферат. Метою роботи є дослідження реакції іоносфери на інтенсивну геомагнітну бурю 27 лютого 2023 року над Харковом та станцією «Академік Вернадський» за допомогою іонозондів. Досліджено поведінку ключових параметрів іоносфери ($h_{m\mathrm{F2}}$ і $N_{m\mathrm{F2}}$) до, під час і після геомагнітної бурі. Проведено порівняння результатів спостережень висоти максимуму шару F2 іоносфери та концентрації електронів на цій висоті з даними, отриманими за допомогою моделі International Reference Ionosphere (IRI-2016). Виявлено значні негативні іоносферні бурі (до ~70% зниження $N_{m\mathrm{F2}}$) над Харковом протягом усіх ночей з початку геомагнітної бурі. Водночас у денні години 27 лютого спостерігалася помірна позитивна іоносферна буря (до ~40% збільшення $N_{m\mathrm{F2}}$). Над станцією «Академік Вернадський» протягом головної фази геомагнітної бурі спостерігалася дуже сильна негативна іоносферна буря (зменшення $N_{m\mathrm{F2}}$ приблизно у 4 рази) як у денні, так і в нічні години. Наведено гіпотези щодо можливих фізичних механізмів (електродинаміка, зміни нейтрального складу, часткове спустошення плазмосфери та зміщення іоносферного провалу), відповідальних за спостережувані іоносферні ефекти. Для виявлення домінуючого драйвера в кожному випадку необхідні подальші досліджня за допомогою фізичних моделей пов'язаних між собою атмосфери, іоносфери та плазмосфери. Порівняння спостережуваних параметрів іоносфери з прогнозами сучасних субмоделей максимуму шару F2 іоносфери моделі IRI свідчить, що $h_{m\mathrm{F2}}$ (AMTB-2013 і SHU-2015), та $N_{m\mathrm{F2}}$ (URSI і CCIR) субмоделі не здатні якісно відтворити зміни в іоносфері, спричинені геомагнітними бурями над Харковом. Над станцією «Академік Вернадський» обидві субмоделі $h_{m\mathrm{F2}}$ недооцінюють висоту максимуму області F2 іоносфери протягом збурених періодів, тоді як субмоделі $N_{m\mathrm{F2}}$ показали кращу чутливість до змін геомагнітної активності. У геомагнітно спокійних умовах якісне узгодження між результатами спостережень та моделювання є задовільним, але для досягнення прийнятної точності кількісних прогнозів потрібні додаткові вдосконалення емпіричних моделей.

Ключові слова: висота максимуму шару F2, геомагнітна буря, емпірична модель, іонозонд, іоносфера, концентрація електронів